# Influence of Residual Water and Cation Acidity on the Ionic Transport Mechanism in Proton-Conducting Ionic Liquids

Jingjing Lin,<sup>a,d</sup> Liming Wang,<sup>b</sup> Tatiana Zinkevich,<sup>c</sup> Sylvio Indris,<sup>c</sup> Yanpeng Suo,<sup>a,d</sup> and Carsten Korte<sup>a,d</sup>\*

- <sup>a</sup> Forschungszentrum Jülich GmbH, Institute of Energy and Climate Research Fuel Cells (IEK-3), 52425 Jülich, Germany
- <sup>b</sup> Central Institute for Engineering, Electronics and Analytics, Analytics (ZEA-3), Jülich, Germany
- <sup>c</sup> Institute for Applied Materials-Energy Storage Systems (IAM-ESS), Karlsruhe Institute of Technology (KIT), 76344 Eggenstein-Leopoldshafen, Germany
- <sup>d</sup> RWTH Aachen University, 52062 Aachen, Germany

#### **Abstract**

Proton-conducting ionic liquids (PILs) are discussed herein as potential new electrolytes for polymer membrane fuel cells, suitable for operation temperatures above 100 °C.1 During fuel cell operation, the presence of significant amounts of residual water is unavoidable, even at theses elevated temperatures. By performing electrochemical and NMR methods, the impact of residual water on 2-Sulfoethylmethylammonium triflate [2-Sema][TfO], 1-Ethylimidazolium triflate [1-EIm][TfO] and Diethylmethylammonium triflate [Dema][TfO] are analyzed. The cationic acidity of these PILs varies by over ten orders of magnitude. Appropriate amounts of the PIL and H<sub>2</sub>O were mixed at various molar ratios to obtain compositions, varying from the neat PIL to H<sub>2</sub>O-excess conditions. The conductivity of [2-Sema][TfO] exponentially increases depending on the H<sub>2</sub>O concentration. The results from <sup>1</sup>H-NMR spectroscopy and self-diffusion coefficient measurements by <sup>1</sup>H field-gradient NMR indicate a fast proton exchange process between [2-Sema]<sup>+</sup> and H<sub>2</sub>O. Conversely, [1-EIm][TfO] and [Dema][TfO] show only a very slow or non-significant, respectively, proton exchange with H<sub>2</sub>O during the time-scale relevant for transport. The proton conduction follows a combination of vehicle and cooperative mechanisms in high acidic PIL, while a mostly vehicle mechanism in medium and low acidic PIL occurs. Therefore, high acidic ionic liquids are promising new candidates for polymer electrolyte fuel cells at an elevated temperature.

#### 1. Introduction

The operation of polymer electrolyte fuel cells (PEFCs) at elevated temperatures of above 100 °C would allow a much simpler system setup: i) no-feed gas humidification; ii) a more efficient cooling system (easier water and heat management); iii) the possibility of recovering high-grade waste heat; and iv) a higher tolerance against feed gas

impurities.<sup>2, 3</sup> The conductivity of proton exchange membranes (PEMs) for low temperature PEFCs, such as NAFION, depends mainly on the uptake of water by the polymer. At elevated temperatures of above 100 °C, a new membrane material should maintain its conductivity in anhydrous conditions. Currently (high temperature), HT-PEFCs are based on phosphoric acid (H<sub>3</sub>PO<sub>4</sub>)-doped polybenzimidazole (PBI) membranes.<sup>4-6</sup> The polymer chains of PBI contain basic functionalities that can be protonated by a strong acid like H<sub>3</sub>PO<sub>4</sub>, forming a charged polymer backbone. Additional molecules of H<sub>3</sub>PO<sub>4</sub> will form a network of hydrogen bonds and additional charge carriers by autoprotolysis, which also provide proton conductivity at lower water concentration.<sup>7</sup>

However, the presence of  $H_3PO_4$  causes a slow cathodic oxygen reduction reaction (ORR) kinetics.<sup>8</sup> This is primarily due to an inhibition (poisoning) effect by the specific adsorption of  $H_3PO_4$  species on active sites of the redox catalyst platinum.<sup>9, 10</sup> Thus, there is a necessity for alternative non-aqueous proton-conducting electrolytes operational for the temperature range between 100–120 °C.

Proton-conducting ionic liquids (PILs) are promising candidates for the use as non-aqueous electrolytes at operation temperatures of above 100 °C. Generally, ionic liquids (IL) are ionic compounds with bulky cations and anions and thus a low lattice energy. Due to their wide electrochemical windows, good conductivity and low flammability, PILs have received much attention for being used as an electrolyte in PEFCs. A PIL consists usually of an (organic) base, protonated by a very strong acid, respecttively a super acid. Anions of super acids such as trifluoromethanesulfonic acid or bis-trifluoromethylsulfonimid have a less inhibiting effect than H<sub>3</sub>PO<sub>4</sub>. The triflate CF<sub>3</sub>SO<sub>3</sub> and the triflimid (CF<sub>3</sub>SO<sub>2</sub>)<sub>2</sub>N anions interact only very weakly with metal atoms, resulting in a weak adsorption on a Pt surface. Anions of super acids such as trifluoromethylsulfonimid have a less inhibiting effect than H<sub>3</sub>PO<sub>4</sub>. The triflate CF<sub>3</sub>SO<sub>3</sub> and the triflimid (CF<sub>3</sub>SO<sub>2</sub>)<sub>2</sub>N anions interact only very weakly with metal atoms, resulting in a weak adsorption on a Pt surface.

A drawback of electrolytes based on ILs or PILs is often poor conductivity because of a comparably high viscosity. In a water-free PIL, protons can only be transported via the protonated cations by means of a vehicle mechanism. A proton transfer back to the anion of the superacid, e.g., [TfO]<sup>-</sup>, does not take place. In this case, conductivity and viscosity are coupled to each other due to the Stokes-Einstein relation. However, PILs in particular, with strong acidic cations, are usually highly hygroscopic. It is difficult to prevent water absorption. Moreover, under fuel cell operation, water will be generated on the cathode side. 19 A steady state concentration of residual water will result from the hygroscopicity of the strongly acidic PIL and the load-dependent water production of the fuel cell. This may offer the possibility to enhance the technically-utilizable conductivity of PIL electrolytes. Water could be regarded as a proton acceptor, a carrier and a donor, and participate in proton transfer process in ionic liquids. This may enable a cooperative transport mechanism. Generally, cooperative proton transport in an IL requires the presence of a proton donor and an acceptor with comparable acidity, see Kreuer et al.<sup>20</sup> Due to the acidity difference between protonated cation and the superacid, a proton transfer back to the anion, e.g. triflate [TfO]-, practically does not take place and thus will not contribute to any cooperative transport.

In this comparative study, the effect of the PIL (cation) acidity on the proton transport mechanism in a system with residual  $H_2O$  is investigated. A highly acidic PIL, 2-Sulfoethylmethylammonum triflate [2-Sema][TfO] (pK<sub>A1</sub>  $\approx$  -1),<sup>19</sup> is compared to a medium acidic PIL, 1-Ethylimidazolium triflate [1-EIm][TfO] (pK<sub>A</sub> = 7.26) and to a low acidic PIL, Diethylmethylammonium triflate [Dema][TfO] (pK<sub>A</sub> = 10.55).<sup>19</sup> The acidity varies over ten orders of magnitude. The 2-Sulfoethylmethylammonium cation is prepared by protonation of 2-Methylaminoethansulfonic acid, which exists as zwitterion due to tautomerism. Because of the presence of sulfonic acid functionality, it is a very strong acid that is able to protonate the residual  $H_2O$  at a significant percentage.<sup>8</sup>

In contrast to the well-known situation of a (diluted) aqueous solution of a salt, where the cations and anions are far outnumbered by the water molecules, only one or two water molecules are present per ion pair if we treat  $IL/H_2O$  systems as mentioned above with less than 10 wt% residual water. There are not enough water molecules available to form a primary solvation sheath. Depending on the properties of cation and anion the water molecules will interact via H bonds or may be accumulated in nano-sized domains.<sup>21, 22</sup> Depending on the acidity of the cation, there will be protolysis reaction with the residual water. If the hydrate of the super acid has an appreciate volatility the presence of water will decrease the thermal stability of the  $PIL.^{8, 19}$ 

Appropriate amounts of the PIL and  $H_2O$  were mixed at various molar ratios to vary the compositions from neat PIL to a (molar) excess of  $H_2O$ . The interactions between the PIL cations and  $H_2O$  were determined by means of electrical conductivity measurements and  $^1H$  NMR spectroscopy. Using a pulsed-field gradient (PFG) NMR technique and the diffusion-ordered spectroscopy (DOSY) technique, the self-diffusion coefficients of the individual protons in the PILs are obtained. The effect of residual  $H_2O$  on the prevailing proton transport mechanism<sup>20</sup> is discussed by comparing the measured macroscopic and microscopic properties.

# 2. Experimental

#### 2.1 Preparation of the used PILs and PIL + H<sub>2</sub>O mixtures

2-Sulfoethylmethylammonum triflate [2-Sema][TfO] was prepared by slowly adding Trifluoromethanesulfonic acid (reagent grade 98%, Sigma Aldrich) to 2-Methylaminoethansulfonic acid (N-Methyltaurine ≥99%, Sigma Life Science). A more detailed description can be found elsewhere.<sup>23</sup> Using Karl-Fischer titration, an initial water content of 0.6 wt% can be found (coulometric mode, 852 Titrando/Metrohm AG).

1-Ethylimidazole triflate [1-EIm][TfO] (CAS No.: 501693-46-5) and Diethylmethylammonium triflate [Dema][TfO] (CAS No.: 945715-39-9), both with a nominal purity of > 98 wt%, were purchased from IoLiTec GmbH. Using Karl-Fischer titration, initial

water contents of 0.2 to 0.25 wt% can be found. In the following a PIL with its the initial (low) water content will be denoted as "neat".

By adding appropriate amounts of  $H_2O$ , a series of mass fractions from 0–7 wt% were obtained. The actual (absolute)  $H_2O$  content was verified by Karl-Fischer titration. In the case of [2-Sema][TfO], a water content of 5.86 wt% corresponds to an equimolar ratio of PIL and  $H_2O$  molecules. In the case of [1-EIm][TfO] and [Dema][TfO], the equimolar ratio is reached at a water content of 6.82 wt% and 7.03 wt%, respectively.

### 2.2 <sup>1</sup>H NMR parameters

The acquisition of the NMR spectra was performed by using a Bruker 600 MHz spectrometer, equipped with a 5 mm cryoprobe tuned to  $^{1}$ H. A capillary filled with D<sub>2</sub>O, included in the sample tubes, was used as a field lock. Measurements of [2-Sema][TfO] and [Dema][TfO] were conducted at room temperature (25 °C), while measurements of [1-EIm][TfO] were conducted at 90 °C.

#### 2.3 Measurement of the Self-diffusion coefficients

The self-diffusion coefficients of the detectable protons were measured by using the PFG/DOSY technique. The measurements of [2-Sema][TfO] at 70 °C were measured by PFG. The  $^1\text{H}$  PFG measurements were performed by a gradient duration of 2 ms; a diffusion time of 50 ms; ns = 32 (number of scans);  $\pi/2$  pulse duration = 17 µsec; recycle delay = 4 s (was defined with T1 saturation recovery beforehand). In the case of  $^{19}\text{F}$  PFG NMR, we used 32 scans for each acquisition, and a recycle delay of = 3 s, the diffusion time and gradient durations were 50 and 2 ms, respectively. The measurements of proton self-diffusion coefficients of [2-Sema][TfO] were repeated at 90 °C by  $^{1}\text{H}$  DOSY. In the cases of [1-EIm][TfO] and [Dema][TfO], the self-diffusion coefficients were also measured by  $^{1}\text{H}$  DOSY. The DOSY measurements were performed by applying 30 gradient increments with a gradient strength (g) from 1.3 to 32.5 G.cm $^{-1}$ . The values of the gradient duration  $\delta$  and diffusion time  $\Delta$  were optimized to obtain at least 85% signal attenuation at the strongest field gradient. The measurements were conducted at 70 and 90 °C, because at lower temperatures the increasing viscosity leads to long relaxation times.

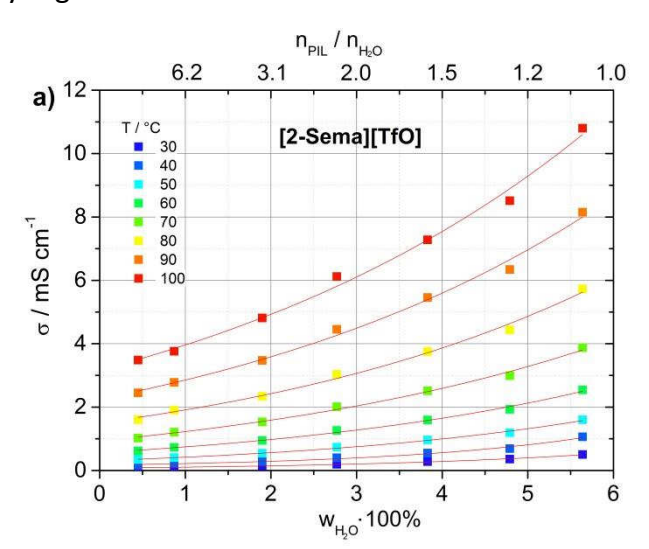
#### 2.4 Conductivity measurement

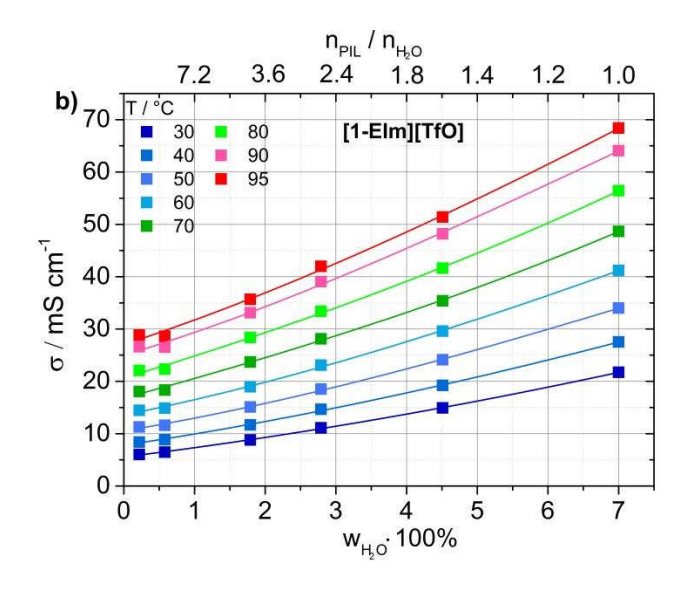
The AC conductivity measurements were performed in a four-probe conductivity cell, using platinum electrodes. The cell constant as a function of the sample volume was determined by using a 0.1 M KCl solution for calibration. The intended  $H_2O$  contents of the binary PIL +  $H_2O$  mixtures were checked by Karl-Fischer titration at the beginning of each measurement. The total ohmic resistance  $\sigma$  as a function of temperature T of the neat PIL and the PIL +  $H_2O$  mixtures was determined by means of impedance spectroscopy. The temperature T was increased in increments of 5 °C from, 30 to 100 °C and vice versa. The excitation amplitude was adjusted to 10 mV for T > 50 °C and to 20 mV for T < 50 °C. The specific conductivity  $\sigma$  is calculated by

#### 3. Results and discussion

#### 3.1 Total conductivity

In Fig. 1, the dependency of the total conductivity  $\sigma$  of [2-Sema][TfO], <sup>19</sup> [1-EIm][TfO] and [Dema][TfO] on the H<sub>2</sub>O content  $w_{\rm H_2O}$  (mass fraction) is depicted. The measurements were performed in the temperature range of between 30 and 100 °C. The total conductivities  $\sigma$  include cationic and anionic charge transport. For all three investigated PILs, this increases as a function of  $w_{\rm H_2O}$ . The highest impact on the total conductivity is found for [2-Sema][TfO], which also has the most acidic cation. <sup>24</sup> At a temperature T of 90 °C, it is increasing by a factor of 3.5 when the H<sub>2</sub>O content rises from approximately 0.45 to 5.7 wt%. There is a non-linear, (quasi-)exponential behaviour. In the case of [1-EIm][TfO] and [Dema][TfO], there are only increases by factors of 2.3 and 1.7, respectively, when increasing the H<sub>2</sub>O content up to about 7 wt%. There is also approximately linear behaviour with [Dema][TfO]. In the case of [1-EIm][TfO], very slight non-linear behaviour can be observed.





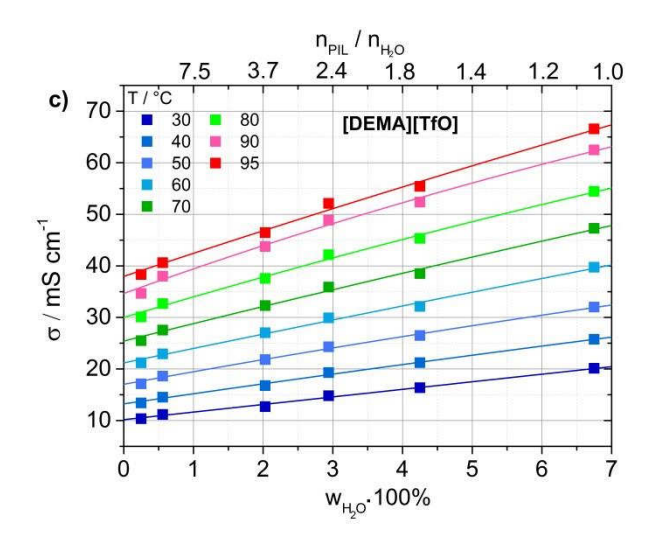


Fig. 1 (Total) conductivity  $\sigma$  of a) [2-Sema][TfO]; b) [1-EIm][TfO]; and c) [Dema][TfO] as a function of the H<sub>2</sub>O content  $w_{\rm H_2O}$  (from nearly neat to equimolar) and temperature T.

#### 3.2 <sup>1</sup>H-NMR / Self-diffusion coefficient

More detailed information on the H $^+$  transport mechanism in the PIL + H $_2$ O systems can be gained by means of  $^1$ H-NMR and PFG NMR/DOSY measurements. The  $^1$ H-NMR spectra of [2-Sema][TfO] and [Dema][TfO] at room temperature (25 °C) and [1-EIm][TfO] at 90 °C at different H $_2$ O contents  $w_{\rm H}_{20}$  are depicted in Fig. 2 a), b) and c). At 25 °C, the signal of the active NH proton in [1-EIm][TfO] is much broader compared to the signals of the alkyl protons and thus hardly detectable. By increasing the temperature, the proton exchange rate becomes faster. This will

narrow the signal (FWHM) of the NH proton. Thus, to gain NMR data for [1-EIm][TfO] that can be evaluated, the measurements were performed at 90 °C. In the cases [2-Sema][TfO] and [Dema][TfO], the number of the detectable proton signals does not change when increasing the temperature T up to 90 °C. There is a slight shift of the H<sub>2</sub>O proton signals and of the N-H proton signal of [Dema][TfO]. Furthermore, at high temperatures the N-H signal starts to decay, as the very fast motion of this species may exceed the monitoring time scale of NMR experiment.

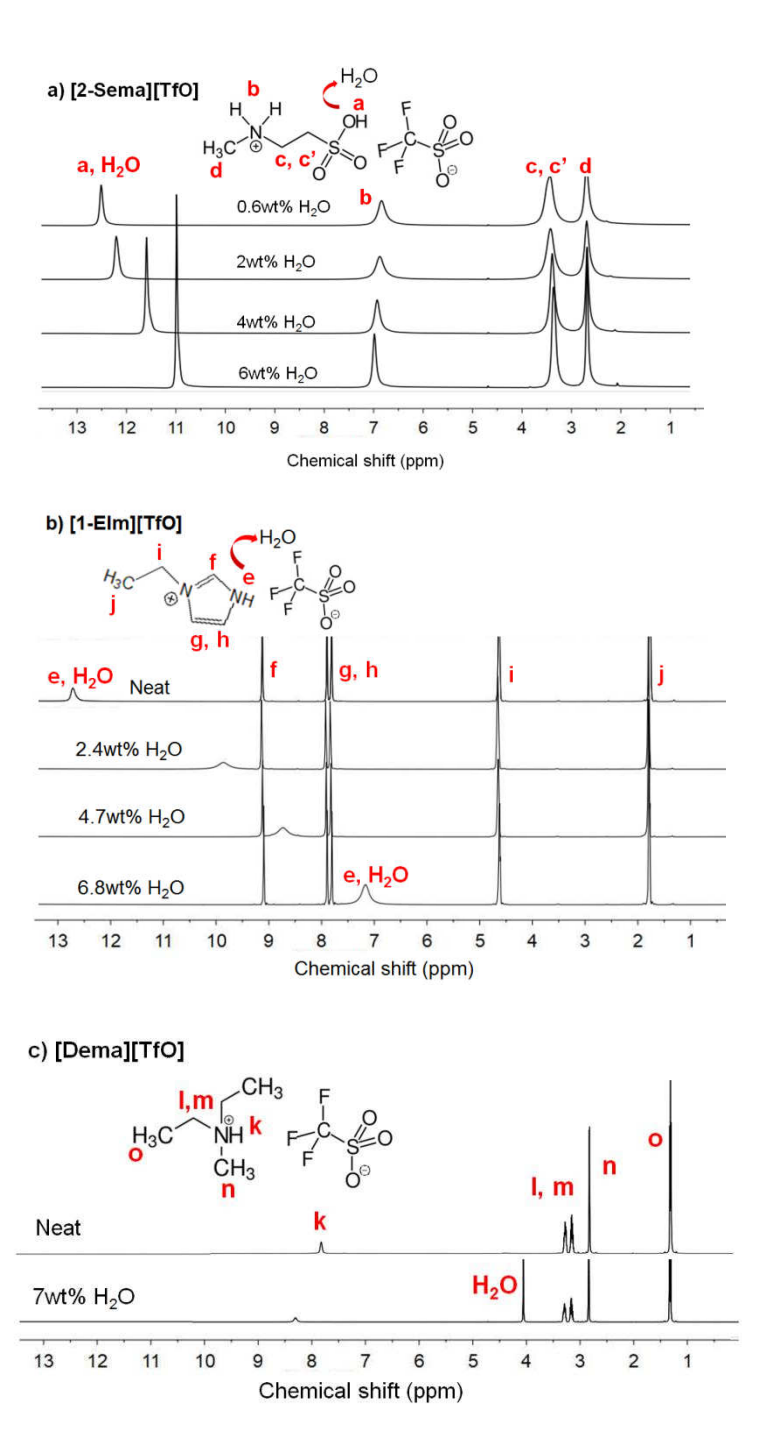


Fig. 2 <sup>1</sup>H NMR spectra of a) [2-Sema][TfO] (T = 25 °C); b) [1-EIm][TfO] (T = 90 °C); and

#### [2-Sema][TfO]

In the case of (nearly) neat [2-Sema][TfO], the protons of the  $NH_2^+$  group show up at 6.83 ppm and of the  $SO_3H$  group at 12.25 ppm; see Fig.2 a). The protons of the  $CH_2CH_2$  backbone are hard to distinguish and can be found at 3.37 ppm, while the protons of the  $CH_3$  group show up at 2.63 ppm. When increasing the  $H_2O$  content up to 6.0 wt%, the signal of the  $SO_3H$  proton shifts by about -1.5 ppm to a higher magnetic field. In the case of the  $NH_2^+$  protons, there is only a slight shift of about +0.2 ppm to a lower magnetic field. Moreover, the signal of the  $SO_3H$  proton shows a corresponding increase in its integral area with an increasing  $H_2O$  amount. This is not the case for the  $NH_2$  and alkyl protons.

Generally, with an increasing concentration of water, it is more probable for the  $H_2O$  molecules to form an H bond to an R-OH or R-NH moiety. The formation of hydrogen bonds will lead to a deshielding of the protons and shift the signal downfield.<sup>25</sup> However, in the <sup>1</sup>H-NMR spectrum of [2-Sema][TfO] +  $H_2O$  mixtures, the signal of the  $H_2O$  protons, which can be expected in the range between 2 and 5 ppm, does not show up at all, independently of the  $H_2O$  concentration. The  $SO_3H$  group of the [2-Sema]<sup>+</sup> cation is a strong proton donor. The protolysis reaction between the [2-Sema]<sup>+</sup> cation and the residual water leads to an intermolecular proton transfer as follows:

CH<sub>3</sub>NH<sub>2</sub><sup>+</sup>CH<sub>2</sub>CH<sub>2</sub>SO<sub>3</sub>**H** + H<sub>2</sub>O 
$$\stackrel{k_1}{\rightleftharpoons}$$
 CH<sub>3</sub>NH<sub>2</sub><sup>+</sup>CH<sub>2</sub>CH<sub>2</sub>SO<sub>3</sub><sup>-</sup> + **H**<sub>3</sub>O<sup>+</sup> (1)

Depending on the water content, also intermolecular proton transfers between  $H_3O^+$  and  $H_2O$ , respectively [2-Sema]<sup>+</sup> and N-Methyltaurine, are possible:

$$H_{3}O^{+} + H_{2}O \xrightarrow{k_{3}} H_{2}O + H_{3}O^{+}$$

$$CH_{3}NH_{2}^{+}CH_{2}CH_{2}SO_{3}H + CH_{3}NH_{2}^{+}CH_{2}CH_{2}SO_{3}^{-} \xrightarrow{k_{4}}$$

$$CH_{3}NH_{2}^{+}CH_{2}CH_{2}SO_{3}^{-} + CH_{3}NH_{2}^{+}CH_{2}CH_{2}SO_{3}H$$
(3)

The pK<sub>A</sub> of hydroxonium cations is equal to  $0.^{*26}$  The pK<sub>A</sub> of the [2-Sema]<sup>+</sup> cation can only be estimated as there is no experimental study available. For the first ionisation constant auf taurine, *i.e.* of the 2-sulfoethylammonium cation, a value of -0.33 is estimated.<sup>27</sup> For ethane sulfonic acids a value of -1.61 can be found.<sup>27, 28</sup> Thus, a

<sup>\*</sup> The equilibrium constant  $K_A$  should be 1 as the activity  $a_{\rm H_2O}$  of water is approximately 1 and the activity of the hydroxonium cations will cancel out in the expression for the mass action law. In the literature also a pK<sub>A</sub> value of -1.74 is found. This value will result when using the concentrations as an approximation for the activities in the mass action law of the protolysis reaction. Merging the (nearly) constant molar concentration of water of 55.5 mol  $I^{-1}$  into the equilibrium constant will yield this value.

value of in the region of -1 seems reasonable. To estimate the equilibrium constant  $K = k_1/k_2$  of the protolysis reaction in Eq. (1), it is surely only a rough approximation to consider the pK<sub>A</sub> values of the involved species, because in fact they can only be applied in diluted aqueous solutions. However, taking only the (estimated) pK<sub>A</sub> values into account, the acidity of the SO<sub>3</sub>H group and the acidity of the H<sub>3</sub>O<sup>+</sup> cation are roughly in the same order of magnitude.

Comparing the estimated pK<sub>A1</sub> value of the cation to the acidity of  $H_3O^+$ , it can be assumed that the rate constants  $k_1$  and  $k_2$  are on the same order of magnitude. If the exchange rates are too fast compared with the spacings of the corresponding peaks in the NMR spectra, the participating species, cations with SO<sub>3</sub>H moiety,  $H_2O$  molecules and  $H_3O^+$  ions, cannot be separated by  $^1H$ -NMR, leading to a signal at an averaged ppm value for the SO<sub>3</sub>H/ $H_2O$  protons. The averaging is weighed by their molar fractions in the equilibrium.  $^{29}$  Depending on solute-solvent interactions, the  $H_3O^+$  protons can be expected between 9.6 and 10.9 ppm and the  $H_2O$  protons between 3.0 and 5.0 ppm, *i.e.*, both at a lower field.  $^{30}$  Despite the deshielding effects of the H-bonds, this may explain why the (averaged) signal of the SO<sub>3</sub>H/ $H_2O$  protons shifts towards lower ppm value (higher fields), when the  $H_2O$  concentration is increased.

In the case of the  $NH_2^+$  protons, the pK<sub>A</sub> value of the  $NH_2^+$  group is several orders of magnitude higher than the pK<sub>A</sub> of  $H_3O^+$  (N-Methyl taurine, pK<sub>A2</sub> = 10.2). <sup>19, 29, 31</sup> Hence, in the protolysis equilibrium with  $H_2O$  molecules, the proton will largely reside on the  $NH_2^+$  group. Thus, due to the slow exchange processes, no significant shift to higher fields can be expected by averaging. An increase in the  $H_2O$  concentration will only increase the (average) number of molecules associated by H bonds, leading to a slight shift to lower magnetic fields. For the other protons of the cation, *i.e.*, the  $CH_2CH_2$  and  $CH_3$  protons, there is no detectable shift as a function of the water concentration.

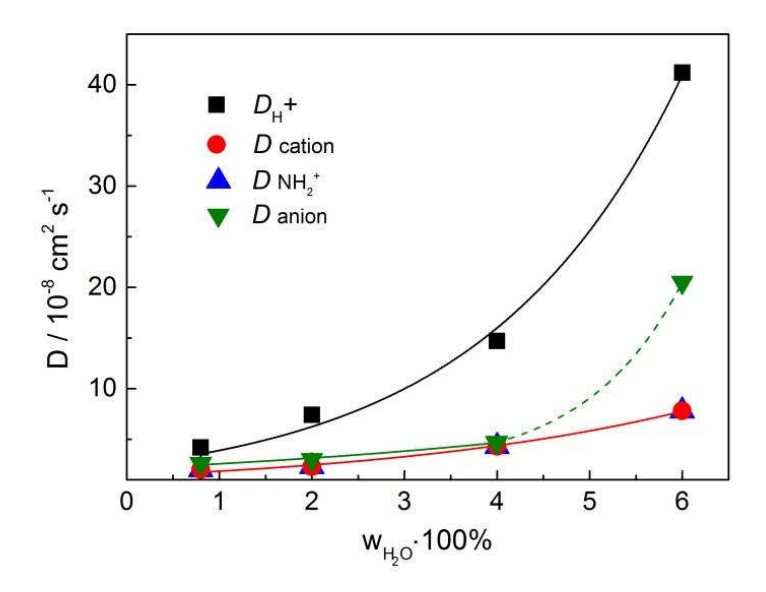


Fig. 3 Self-diffusion coefficients of the SO<sub>3</sub>H/H<sub>2</sub>O ( $\equiv D_{H^+}$ ), the NH<sub>2</sub>, the CH<sub>n</sub> protons

measured for [2-Sema][TfO] at 70 °C with various  $H_2O$  contents  $w_{H_2O}$  obtained from  $^1H$  and  $^{19}F$ -NMR PFG measurements. (The diffusion coefficients of  $CH_3$  and  $CH_2CH_2$  cannot be separated because of a limited resolution at lower fields spectrometer (300MHz).

These observations were confirmed by  $^1$ H and  $^{19}$ F-NMR PFG measurements. This technique allows for the determination of the self-diffusion coefficient  $D_i$  attributed to a certain protonic species i in the spectrum.  $^{32}$  An PFG spectrum of [2-Sema][TfO] at 90  $^{\circ}$ C and an equimolar content of  $H_2$ O is shown in Fig. 4 a). The evaluated diffusion coefficients  $D_i$  for the individual protons at 70  $^{\circ}$ C and various  $H_2$ O contents  $w_{H_2O}$  are shown in Fig. 3 and listed Tab 1 a). Because of the high viscosity of [2-Sema][TfO], the PFG measurements were performed at elevated temperatures.

For all of the measured samples, the diffusion coefficients of the  $CH_n$  and the  $NH_2^+$  protons, *i.e.*,  $D_{CH_3}$ ,  $D_{CH_2CH_2}$  and  $D_{NH_2^+}$ , are nearly equal; see also Fig. 4 a). Thus, they should be identical to the diffusion coefficient  $D_{Sema^+}$  of the cation and, respectively, to the diffusion coefficient  $D_{H^+,vehicle}$  of the active protons by means of the vehicular mechanism. The  $SO_3H/H_2O$  protons are significantly more mobile than all of other protons of the cation, *i.e.*, more mobile than the cation:

$$D_{\text{SO}_3\text{H/H}_2\text{O}} \gg D_{\text{NH}_2^+} \approx D_{\text{CH}_n} \equiv D_{\text{2-Sema}^+} \equiv D_{\text{H}^+,\text{vehicle}}$$
 (4)

The self-diffusion coefficients of the individual protons show a strong dependence on  $w_{\rm H_2O}$ . A (quasi-)exponential increase can be observed in Fig. 3.

Considering also the strong shift of the  $SO_3H/H_2O$  NMR signal in Fig. 2 as a function of the water content  $w_{H_2O}$ , the increase of the mobility of the  $SO_3H/H_2O$  protons compared to the other protons is most probably due to fast proton exchange processes with the  $H_2O$  molecules and a higher mobility of the  $H_3O^+$  ions; see equilibrium in Eq. (1). An upcoming cooperative transport mechanism for the protons can also be taken into account and involves the exchange processes in Eq. (3) and (4). The slight increase of the self-diffusion coefficients  $D_{2-Sema}^+$  of the cation may be caused by a decrease in the viscosity of the PIL due to the increasing water content. The diffusion of the  $SO_3H/H_2O$  protons is responsible for the electrochemical proton transport. The diffusion coefficient  $D_{SO_3H/H_2O}$  of the  $SO_3H/H_2O$  protons should be identical to the diffusion coefficient  $D_{H^+}$  of all the active protons:

$$D_{\mathrm{SO_3H/H_2O}} \equiv D_{\mathrm{H}^+} \tag{5}$$

The diffusion coefficient  $D_{\rm H^+}$  of all the active protons should be a sum of the diffusion coefficients of the active protons  $D_{\rm H^+,vehicle}$  by means of the vehicular

mechanism (i.e., of the cations  $D_{2\text{-Sema}^+}$ ) and the active protons  $D_{\text{H}^+,\text{coop}}$  by the cooperative mechanism, see also Nakamato et al:<sup>33</sup>

$$D_{\mathrm{H}^{+}} = D_{\mathrm{H}^{+},\mathrm{vehicle}} + D_{\mathrm{H}^{+},\mathrm{coop}} \tag{6}$$

The diffusion coefficient  $D_{\rm TfO^-}$  of the triflate anions were determined by performing  $^{19}$ F-NMR PFG measurements. If the concentration  $c_{\rm H^+}$  and  $c_{\rm TfO^-}$  of the mobile protonic and anionic charge carriers are equal, the transference number  $t_{\rm H^+}$  of the protons can be calculated solely from the diffusion coefficients  $D_{\rm H^+}$  and  $D_{\rm TfO^-}$ . This assumption is also valid in the case of a protolysis equilibrium with water:

$$t_{\rm H^+} = \frac{\sigma_{\rm H^+}}{\sigma_{\rm total}} = \frac{\sigma_{\rm H^+}}{\sigma_{\rm H^+} + \sigma_{\rm Tf0^-}} = \frac{D_{\rm H^+} c_{\rm H^+}}{D_{\rm H^+} c_{\rm H^+} + D_{\rm Tf0^-} c_{\rm Tf0^-}} \approx \frac{D_{\rm H^+}}{D_{\rm H^+} + D_{\rm Tf0^-}}$$
(7)

The measured data for the diffusion coefficient  $D_{\rm TfO^-}$  of the triflate anion is shown in Fig. 3 and Table 1 a). The transference numbers  $t_{\rm H^+}$  according to Eq. (7) and the resulting partial proton conductivity  $\sigma_{\rm H^+}=t_{H^+}\,\sigma_{\rm total}$  is also listed in Table 1.

The content of residual water  $w_{\rm H_2O}$  could not be decreased below 0.8 wt% due to the experimental limitations in this study. When (exponentially) extrapolating the diffusion coefficients for the acidic SO<sub>3</sub>H/H<sub>2</sub>O protons  $D_{\rm H^+}$ , the other protons of the cation  $D_{\rm Sema^+}$  and the triflate anion  $D_{\rm TfO^-}$ , they converge approximately to the same value when reaching the ordinate. This observation can be explained if a pure vehicle mechanism for proton transport is present in the neat PIL, *i.e.*, if  $w_{\rm H_2O} = 0.0$  wt%. Thus, a self-diffusion coefficient  $D_{\rm H^+,vehicle}$  ( $\equiv D_{\rm 2-Sema^+}$ ) of  $(2.0\pm0.5)\cdot 10^{-8}$  cm<sup>2</sup> s<sup>-1</sup> for pure vehicular transport proton transport in the neat PIL at 70 °C can be estimated. The transference number  $t_{\rm H^+}$  is then approaching a value of approximately ½.

Moreover, in the composition range of up to 4 wt%  $\rm H_2O$ , the diffusion coefficients of the cation  $D_{\rm 2-Sema^+}$  and the triflate anion  $D_{\rm TfO^-}$  are nearly identical. As expected for a change from a vehicular to a cooperative proton transport mechanism, the transference number  $t_{\rm H^+}$  is increasing, reaching a value of 76%. When increasing the water content from 4 to 6 wt%, the transference number  $t_{\rm H^+}$  decreases again due to an enhanced increase in the anionic diffusion coefficient  $D_{\rm TfO^-}$ . This may be caused by a smaller molecular radius of the triflate anion compared to [2-Sema]<sup>+</sup> cation. An increasing solvation may in turn reduce an association between cations and anions (ion pairs). As a result, the diffusion coefficients of the cation and anion may diverge and the different molecular sizes will matter. Similar results are reported by Hou et al.<sup>34</sup> In addition, the hydrophilic triflate anion may lead to a decrease in the microviscosity, also providing a faster diffusion of anions.<sup>25</sup>

Tab. 1 a) Diffusion coefficients,  $t_{\rm H+}$  and  $\sigma_{\rm H+}$  in [2-Sema][TfO] + H<sub>2</sub>O at 70 °C.

$w_{ m H_2O}$	$D_{\mathrm{H}^+}$	$D_{2\text{-Sema}}$ +	$D_{ m TfO}$ –	$t_{ m H^+}$	$\sigma_{ ext{H}}$ +	

wt%	10 <sup>-8</sup> cm <sup>2</sup> S <sup>-1</sup>	10 <sup>-8</sup> cm <sup>2</sup> S <sup>-1</sup>	10 <sup>-8</sup> cm <sup>2</sup> S <sup>-1</sup>		10 <sup>-4</sup> S cm <sup>-1</sup>
0.0*	2.3 ± 0.3	1.4 ± 0.1	2.1 ± 0.2	0.52	0.52
0.8	4.20 ± 0.01	2.00±0.01	2.60±0.03	0.62	7.47
2	7.40 ± 0.01	2.30±0.01	3.00±0.03	0.71	11.0
4	14.7 ± 0.03	4.10±0.02	4.70±0.05	0.76	19.3
6	41.2 ± 0.09	7.60±0.04	20.5±0.2	0.67	27.4

<sup>\*</sup> Extrapolated data for  $\,D_{
m H^+},\,\,D_{
m 2-Sema^+}\,$  and  $\,D_{
m TfO^-}$ 

Tab. 1 b) Diffusion coefficients and  $D_{H^+,coop}/D_{H^+}$  in [2-Sema][TfO] + H<sub>2</sub>O at 90 °C.

$w_{\rm H_2O}$	$D_{\mathrm{H}}$ +	D <sub>2-Sema</sub> +	$D_{\mathrm{H^+,coop}}/D_{\mathrm{H^+}}$
wt%	10 <sup>-5</sup> cm <sup>2</sup> S <sup>-1</sup>	10 <sup>-5</sup> cm <sup>2</sup> S <sup>-1</sup>	
6.0	0.56	0.17	0.70

Tab. 1 c) Diffusion coefficients and  $D_{\rm H^+,coop}/D_{\rm H^+}$  in [1-EIm][TfO] + H<sub>2</sub>O at 90 °C.

$w_{\mathrm{H}_2\mathrm{O}}$	$D_{\mathrm{H}}{}^{+}$	D <sub>2-Sema</sub> +	$D_{\mathrm{H^+,coop}}/D_{\mathrm{H^+}}$
wt%	10 <sup>-5</sup> cm <sup>2</sup> S <sup>-1</sup>	10 <sup>-5</sup> cm <sup>2</sup> S <sup>-1</sup>	
6.8	17.1	12.4	0.27

Tab. 1 d) Diffusion coefficients and  $D_{\rm H^+,coop}/D_{\rm H^+}$  in [Dema][TfO] + H<sub>2</sub>O at 30 °C.

$w_{\rm H_2O}$	$D_{\mathrm{H}}$ +	$D_{2 ext{-Sema}}$ +	$D_{\mathrm{H}^+,\mathrm{coop}}/D_{\mathrm{H}^+}$
wt%	10 <sup>-5</sup> cm <sup>2</sup> S <sup>-1</sup>	10 <sup>-5</sup> cm <sup>2</sup> S <sup>-1</sup>	
7.0	1.13	1.12	~0

The self-diffusion coefficient  $D_{\rm H^+}$  ( $\equiv D_{\rm SO_3H/H_2O}$ ) of all active protons should be connected by the Nernst-Einstein equation to the (partial) proton conductivity  $\sigma_{\rm H^+}$  if there is an uncorrelated motion of the protons:

$$\frac{D_{\rm H} + c_{\rm H}^{+}}{RT} = \frac{\sigma_{\rm H}^{+}}{F^2} \tag{8}$$

The molar concentration of the mobile H<sup>+</sup> ions is denoted with  $c_{\rm H^+}$ . It can be calculated from the mass fraction  $w_{\rm H_2O}$  using the molar weight  $M_{\rm 2-SemaTfO}$  and the density  $\rho$  (of the mixture)<sup>†</sup>:

\_

 $<sup>^{\</sup>scriptscriptstyle +}$  Consider  $w_{\text{2-SemaTfO}} + w_{\text{H}_2\text{O}} = 1$ 

$$c_{\rm H^+} = (1 - w_{\rm H_2O}) \frac{\rho}{M_{\rm 2-SemaTfO}} \tag{9}$$

A density of 1.61 g cm<sup>-1</sup> can be measured for the neat PIL at 70 °C. <sup>23</sup> In the case of a diffusion coefficient  $D_{\rm H^+}$  of about  $(2.0\pm0.5)\cdot 10^{-8}$  cm<sup>2</sup> s<sup>-1</sup> this results in a partial cationic conductivity of  $(0.36\pm0.09)$  mS cm<sup>-1</sup>. Using the extrapolated value of the total conductivity at  $w_{\rm H_2O}$  = 0 wt% of about 1.0 mS cm<sup>-1</sup>, it yields a transference number  $t_{\rm H^+}$  of the protonic charge carriers of about  $(36\pm9)$  %. This is lower compared to the value obtained when employing the <sup>19</sup>F-NMR PFG data (~50 %), but when considering the experimental errors is still in a comparable range.

## [1-EIm][TfO]

In the case of (nearly) neat [1-EIm][TfO], the protons of the acidic NH moiety show up at 12.71 ppm; see Fig. 2 b). The CH protons of the imidazolium ring can be found at 9.07, 7.87 and 7.79 ppm. The signals of the  $CH_2$  and  $CH_3$  protons of the ethyl group are at 4.61 and 1.78 ppm. When increasing the  $H_2O$  content up to 6.8 wt%, the signal of the NH protons shifts about -5.5 ppm to a higher magnetic field, down to 7.1 ppm.

As observed for [2-Sema][TfO] +  $H_2O$  mixtures, the signal of the  $H_2O$  protons does not show up independently in the  $H_2O$  concentration. There is also a protolysis equilibrium of the [1-EIm]<sup>+</sup> cation and residual  $H_2O$ . The pK<sub>A</sub> value of the [1-EIm]<sup>+</sup> cation is several orders of magnitude higher than the pK<sub>A</sub> of  $H_3O^+$ :

CH=NH<sup>+</sup>-CH=CH-N(C<sub>2</sub>H<sub>5</sub>) + H<sub>2</sub>O
$$\underset{k_2}{\overset{k_1}{\rightleftharpoons}}$$
 CH=N-CH=CH-N(C<sub>2</sub>H<sub>5</sub>) + H<sub>3</sub>O<sup>+</sup> (10)

Using the pK<sub>A</sub> data to estimate the equilibrium constant  $K=k_1/k_2$  yields a value on the order of  $10^{-7}$ . This implies that the rate constants are very different, *i.e.*,  $k_1 < k_2$ , but the exchange rate  $k_1$  is still too fast compared to the NMR sampling frequency. This results again in an averaged ppm value of the NH signal and no separate water signal.

As the fast proton exchange takes place between the acidic moiety of the cation,  $H_2O$  and  $H_3O^+$ , and the averaging is weighed by their molar fractions, the equilibrium concentrations of these species must be considered. The acidity of the arylic NH moiety in [1-Elm][TfO] is significantly lower compared to  $SO_3H$  moiety in [2-Sema][TfO]. Thus, in the system [1-Elm][TfO] +  $H_2O$ , there will only be significant molar fractions of the [1-Elm] $^+$  cations and  $H_2O$ . In the system [2-Sema][TfO] +  $H_2O$ , a substantial molar fraction of  $H_3O^+$  is also present. The  $H_3O^+$  protons can be expected at a lower field (~9.60 ppm) than the  $H_2O$  protons (3.0 to 5.0 ppm). This may lead to a stronger high-field shift of the averaged signal of the acidic proton in the system [1-Elm][TfO] +  $H_2O$  compared to the system [2-Sema][TfO] +  $H_2O$ , when increasing the water concentration. <sup>29</sup> Similar averaged chemical shifts are reported by Yaghini et al. <sup>35</sup> Meanwhile, the good overlap between the calculated population-averaged

chemical shift of NH and  $H_2O$  and the observed NH/  $H_2O$  chemical shift indicates the exchange between  $H_2O$  and NH, and rarely the existence of  $H_3O^+$ .<sup>36</sup>

At temperatures below 90 °C, the proton exchange rate in the system [1-EIm][TfO] +  $H_2O$  and, respectively, the corresponding spin-spin relaxation time  $T_2$  of the NH/ $H_2O$  proton is too small. Only at elevated temperature does the accelerated exchange process provide a detectable but still broad signal. Compared to the narrow signal of the  $SO_3H/H_2O$  proton in the system [2-Sema][TfO] +  $H_2O$ , even at room temperature, it can be inferred that the proton exchange rate in the system [1-EIm][TfO] +  $H_2O$  is much slower.

The  $^1\text{H-DOSY}$  2-D spectrum of [1-EIm][TfO] at a temperature of 90 °C and an equimolar content of  $\text{H}_2\text{O}$  is shown in Fig. 4 b). The evaluated diffusion coefficients are listed in Table 1 c). As observed for [2-Sema][TfO], the diffusion coefficients of the non-acidic protons of the [1-EIm]+ cation are nearly equal, *i.e.*, the CH protons of the imidazole ring, the CH<sub>2</sub> and CH<sub>3</sub> protons of the ethyl group. Thus, they should be identical to the diffusion coefficient  $D_{\text{1-EIm}}+$  of the cation to the diffusion coefficient  $D_{\text{H}^+,\text{vehicle}}$  of the active protons by the vehicular mechanism, respectively, with a value of  $1.24 \cdot 10^{-4} \text{ cm}^2 \text{ s}^{-1}$  found. The NH/H<sub>2</sub>O protons are significantly more mobile than the other protons of the cation:

$$D_{\rm NH/H_2O} \gg D_{\rm 1-EIm^+} \equiv D_{\rm H^+, vehicle} \tag{11}$$

The diffusion coefficient  $D_{\rm NH/H_2O}$  of NH/H<sub>2</sub>O protons should be identical to the diffusion coefficient  $D_{\rm H^+}$  of all active protons:

$$D_{\rm NH/H_2O} \equiv D_{\rm H^+} \tag{12}$$

A value of  $1.71 \cdot 10^{-4} \, \mathrm{cm^2 \, s^{-1}}$  is measured. As is given in Eq. (6), the diffusion coefficient  $D_{\mathrm{H^+}}$  should be a sum of the diffusion coefficients of the active protons  $D_{\mathrm{H^+,vehicle}}$  by the vehicular mechanism (*i.e.*,  $D_{\mathrm{1-Elm^+}}$ ) and the active protons  $D_{\mathrm{H^+,coop}}$  by the cooperative mechanism. Thus,  $D_{\mathrm{H^+,coop}}$  yields  $4.7 \cdot 10^{-5} \, \mathrm{cm^2 \, s^{-1}}$ .

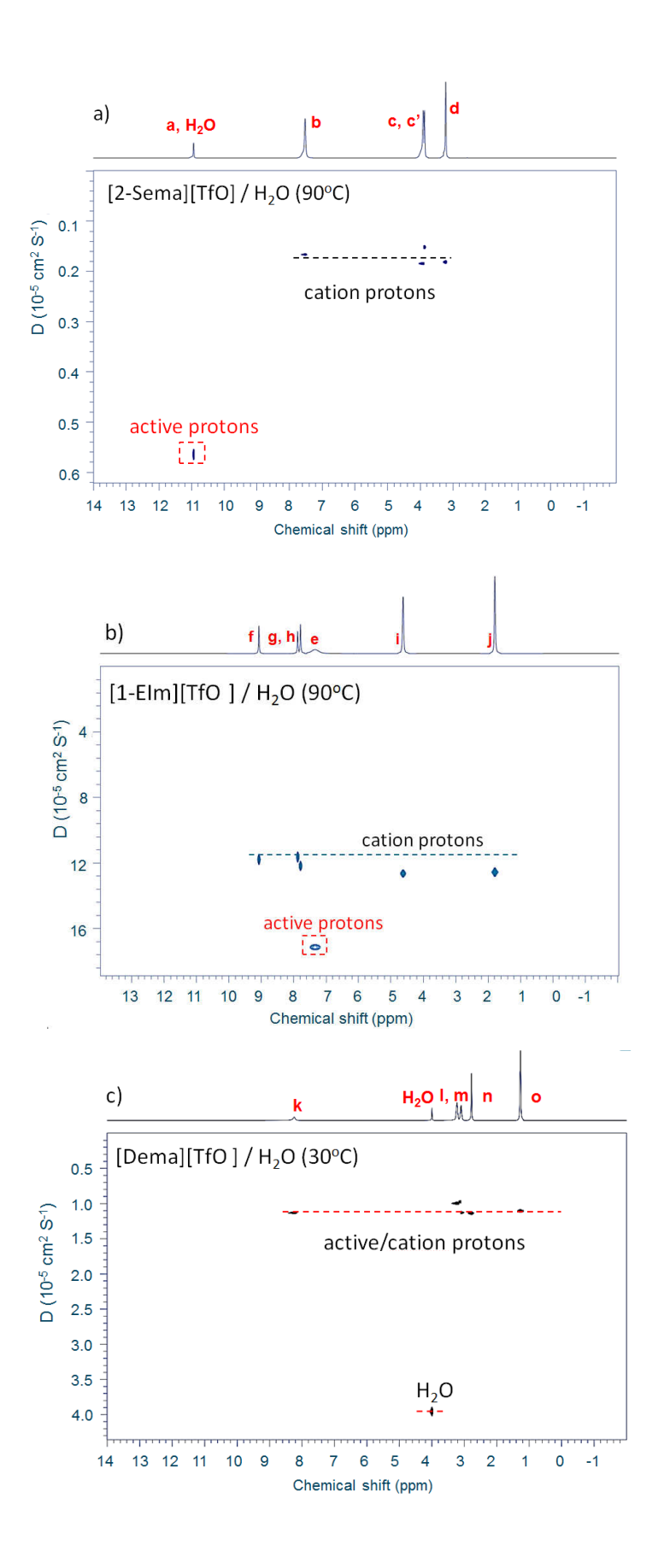


Fig. 4  $^{1}$ H-DOSY 2D spectra of a) [2-Sema][TfO] + 6.0 wt% H<sub>2</sub>O; b) [1-EIm][TfO] + 6.8 wt% H<sub>2</sub>O; and c) [Dema][TfO] + 7.0 wt% H<sub>2</sub>O at different temperatures. The H<sub>2</sub>O content is

#### [Dema][TfO]

In the case of low acidic [Dema][TfO] at 30 °C, in the neat PIL the signal at 7.80 ppm in the  $^1\text{H-NMR}$  spectrum can be assigned to the NH proton. The CH<sub>3</sub> protons of the methyl group can be found at 2.83 ppm and the signals of the CH<sub>2</sub> and CH<sub>3</sub> protons of the ethyl group are at 3.18/3.31 and 1.34 ppm, respectively. With the increasing H<sub>2</sub>O concentration, up to an equimolar composition (7.0 wt%), the signal the NH protons shifts by about 0.5 ppm towards a lower field of up to 8.26 ppm. The signal of the H<sub>2</sub>O protons can be identified in the neat PIL and at higher H<sub>2</sub>O concentrations. The acidity of the [Dema]<sup>+</sup> cation is about three orders of magnitude smaller than the [1-Elm]<sup>+</sup> cation and about ten orders less than the [2-Sema]<sup>+</sup> cation:

$$CH_3(CH_3CH_2)_2NH^+ + H_2O \underset{k_2}{\overset{k_1}{\rightleftharpoons}} CH_3(CH_3CH_2)_2N + H_3O^+$$
 (13)

Using the pK<sub>A</sub> data to estimate the equilibrium constant  $K = k_1/k_2$  of the protolysis equilibrium with H<sub>2</sub>O yields a value on the order of  $10^{-10}$ . It seems that in the system [Dema][TfO] + H<sub>2</sub>O, the proton largely resides on the amine-N during the NMR sampling process. No shift to higher fields can be detected due to an extremely slow proton exchange rate  $k_1$  between the cation and H<sub>2</sub>O. An increase in the H<sub>2</sub>O concentration will only increase the (average) number of molecules associated by H bonds, leading to the observed slight shift of the NH/H<sub>2</sub>O protons to lower magnetic fields.

The  $^1\text{H-DOSY}$  2-D spectrum of [Dema][TfO] and an equimolar  $\text{H}_2\text{O}$  are shown in Figure 4 c) and the self-diffusion coefficients are listed in Table 1 d). In order to avoid eddying effects due to viscosity at high temperatures being too low, the PFG/DOSY measurement of [Dema][TfO] was performed at room temperature. The diffusion

coefficient  $D_{\rm NH/H_2O}$  of the NH/H<sub>2</sub>O protons has the same value as the other protons

of the cation [Dema]<sup>+</sup> cation, because there is no fast proton exchange with  $H_2O$  molecules. Thus, it has to be identical to the diffusion coefficient  $D_{\rm H^+,vehicle}$  for vehicular proton transport. This also confirms the conclusions stated above. A value

of 1.1 
$$\cdot$$
 10<sup>-5</sup> cm² s<sup>-1</sup> is obtained. Correspondingly, the diffusion coefficient  $D_{
m H^+,coop}$ 

for cooperative proton transport has to be zero. This was also observed by Yaghini et al.  $^{35}$  for the Diethylmethylammonium methanesulfonate [Dema][MsO]. In the case of this PIL, the cooperative proton transfer mechanism does also not contribute, independently of the  $H_2O$  concentration.

The protons of the  $H_2O$  molecules diffuse more rapidly than cations due to the smaller molecule diameter. A value of  $3.81 \cdot 10^{-5} \, \text{cm}^2 \, \text{s}^{-1}$  is measured, but this will not contribute to the electrochemical proton conduction.

Cooperative vs. vehicular proton transport

The neat PILs (electrochemical) proton transport can only take place by means of a vehicular mechanism, as proton transfers from the cation back to the anion are highly improbable due to the large difference in acidity between the conjugated acid and cation. For each investigated PIL, the increase in the cation diffusion coefficient and thus of the diffusion coefficient  $D_{\rm H^+,vehicle}$  of vehicular transport are caused by a decrease in the viscosity when increasing the H<sub>2</sub>O content  $w_{\rm H_2O}$  (Stokes-Einstein relation).

The ratio of cooperative diffusion  $D_{\rm H^+,coop}$  to the total diffusion  $D_{\rm H^+}$  of the active protons can be calculated as follows:

$$\frac{D_{\rm H^+,coop}}{D_{\rm H^+}} = \frac{D_{\rm H^+} - D_{\rm H^+,vehicle}}{D_{\rm H^+}}$$
 (14)

The diffusion coefficient  $D_{\mathrm{H^+,vehicle}}$  of the (active) protons by vehicular transport can also be identified for all investigated PILs as being identical to the diffusion coefficient of the cation, i.e.,  $D_{2\text{-Sema}^+}$   $D_{1\text{-EIm}^+}$  and  $D_{\mathrm{Dema}^+}$ . The results for the systems [2-Sema][TfO] + H<sub>2</sub>O and [1-EIm][TfO] + H<sub>2</sub>O at 90 °C and for [Dema][TfO] + H<sub>2</sub>O at room temperature are shown in Table 1 b) to d), each with an equimolar amount of H<sub>2</sub>O.

The ratio  $D_{\rm H^+,coop}/D_{\rm H^+}$  yields 0.70 in the case of [2-Sema][TfO] + H<sub>2</sub>O and 0.28 for [1-EIm][TfO] + H<sub>2</sub>O and ~0% for [Dema][TfO] + H<sub>2</sub>O. These findings confirm the assumption regarding the proton transport mechanisms that was made in the preceding subsections, namely that a higher acidity of the cation leads to a more pronounced protolysis and faster proton exchange with the residual water and thus to a higher share of cooperative transport. In the system [2-Sema][TfO] + H<sub>2</sub>O, the equilibrium concentration of  $H_3O^+$  is significantly higher than in [1-EIm][TfO] +  $H_2O$ . Thus, in the system [Dema][TfO] + H<sub>2</sub>O, the (quasi-)linear increase of the total conductivity  $\sigma$  vs. the H<sub>2</sub>O content  $w_{\rm H_2O}$  is only caused by a decrease in the viscosity and a faster diffusion of the cations, providing solely vehicular proton transport. In the system of [1-EIm][TfO] + H<sub>2</sub>O, the relatively slow proton exchange rate between cation and H<sub>3</sub>O<sup>+</sup> is not sufficient for a predominating cooperative proton transfer. However, in the system [2-Sema][TfO] + H<sub>2</sub>O, with the highest cation acidity, a change from vehicular to a predominating cooperative proton transport can be observed. This may lead to (quasi-)exponential behaviour of the total conductivity  $\sigma$  vs.  $w_{\rm H_2O}$  for this system.

#### 4. Conclusion

Proton-conducting ionic liquids (PIL) with triflate anions and cations with various acidity and a residual water content of up to 7 wt% were investigated regarding proton conductivity and self-diffusion by following electrochemical and NMR methods. The predominating proton transfer mechanism depends on both the cation acidity and residual water content. In the case of [Dema][TfO], with very low cation acidity, only vehicular transport was found across the entire investigated concentration range. With increasing cation acidity, in the case of [1-EIm][TfO] and [2-Sema][TfO], an increasing fraction of cooperative proton transport can be observed. In the highly acidic PIL [2-Sema][TfO], cooperative transport prevails for H<sub>2</sub>O contents of 6 wt%, resulting in a strong increase in the conductivity. Thus, for future use as electrolytes in polymer membrane fuel cells for elevated temperatures (100–120 °C) and atmospheric operation, the cathodic formation of H<sub>2</sub>O favours the use of PILs with high acidic cations and high hygroscopicity. Enabling fast cooperative transport may help reach sufficient proton conductivities during operation.

# 1. Y. Liu, W. Lehnert, H. Janßen, R. C. Samsun and D. Stolten, *Journal of Power Sources*, 2016, **311**, 91-102.

- 2. D. J. Jones and J. Rozière, Journal of Membrane Science, 2001, 185, 41-58.
- 3. E. Quartarone and P. Mustarelli, Energy & Environmental Science, 2012, 5, 6436-6444.
- 4. Q. Li, J. O. Jensen, R. F. Savinell and N. J. Bjerrum, *Progress in polymer science*, 2009, **34**, 449-477.
- 5. J. A. Asensio, E. M. Sánchez and P. Gómez-Romero, *Chemical Society Reviews*, 2010, **39**, 3210-3239.
- 6. L. Vilčiauskas, M. E. Tuckerman, G. Bester, S. J. Paddison and K.-D. Kreuer, *Nature chemistry*, 2012, **4**, 461.
- 7. C. Korte, F. Conti, J. Wackerl, P. Dams, A. Majerus and W. Lehnert, *Journal of Applied Electrochemistry*, 2015, **45**, 857-871.
- 8. K. Wippermann, J. Wackerl, W. Lehnert, B. Huber and C. Korte, *Journal of The Electrochemical Society*, 2015, **163**, F25-F37.
- 9. K. Hsueh, E. Gonzalez and S. Srinivasan, *Electrochimica Acta*, 1983, **28**, 691-697.
- 10. K. L. Hsueh, E. Gonzalez, S. Srinivasan and D. T. Chin, *Journal of the Electrochemical Society*, 1984, **131**, 823-828.
- 11. A. Noda, M. A. B. H. Susan, K. Kudo, S. Mitsushima, K. Hayamizu and M. Watanabe, *The Journal of Physical Chemistry B*, 2003, **107**, 4024-4033.
- 12. M. A. B. H. Susan, T. Kaneko, A. Noda and M. Watanabe, *Journal of the American Chemical Society*, 2005, **127**, 4976-4983.
- 13. M. M. Mannarino, D. S. Liu, P. T. Hammond and G. C. Rutledge, *ACS applied materials & interfaces*, 2013, **5**, 8155-8164.
- 14. D. E. Smith and D. A. Walsh, Advanced Energy Materials, 2019, 9.
- 15. L. Koók, B. Kaufer, P. Bakonyi, T. Rózsenberszki, I. Rivera, G. Buitrón, K. Bélafi-Bakó and N. J. J. o. m. s. Nemestóthy, 2019, **570**, 215-225.
- 16. J. Escorihuela, A. Garcia-Bernabe, A. Montero, O. Sahuquillo, E. Gimenez and V. Compan, *Polymers (Basel)*, 2019, **11**.

- 17. P. Zelenay, B. Scharifker, J. M. Bockris and D. Gervasio, *Journal of the Electrochemical Society*, 1986, **133**, 2262-2267.
- 18. V. S. Murthi, R. C. Urian and S. Mukerjee, *The Journal of Physical Chemistry B*, 2004, **108**, 11011-11023.
- 19. K. Wippermann, J. Giffin and C. Korte, *Journal of The Electrochemical Society*, 2018, **165**, H263-H270.
- 20. K. D. Kreuer, A. Rabenau and W. J. Weppner, *Angewandte Chemie International Edition in English*, 1982, **21**, 208-209.
- 21. L. Suo, O. Borodin, Y. Wang, X. Rong, W. Sun, X. Fan, S. Xu, M. A. Schroeder, A. V. Cresce, F. Wang, C. Yang, Y.-S. Hu, K. Xu and C. Wang, *Advanced Energy Materials*, 2017, **7**.
- 22. Y. Zhang, R. Ye, D. Henkensmeier, R. Hempelmann and R. Chen, *Electrochimica Acta*, 2018, **263**, 47-52.
- 23. K. Wippermann, J. Giffin, S. Kuhri, W. Lehnert and C. Korte, *Physical Chemistry Chemical Physics*, 2017, **19**, 24706-24723.
- 24. J. Wainright, J. T. Wang, D. Weng, R. Savinell and M. Litt, *Journal of the Electrochemical Society*, 1995, **142**, L121-L123.
- 25. T. A. Fadeeva, P. Husson, J. A. DeVine, M. F. Costa Gomes, S. G. Greenbaum and E. W. Castner, Jr., *J Chem Phys*, 2015, **143**, 064503.
- 26. E. C. Meister, M. Willeke, W. Angst, A. Togni and P. Walde, *Helvetica Chimica Acta*, 2014, **97**, 1-31.
- 27. E. J. King, Journal of the American Chemical Society, 1953, **75**, 2204-2209.
- 28. H. Huang, J. Y. Jin, J.H. Hong, J.S. Kang and W. Lee, *Bulletin of the Korean Chemical Society*, 2009, **30**, 2827-2829.
- 29. P. Rimmelin, S. Schwartz and J. Sommer, *Organic Magnetic Resonance*, 1981, **16**, 160-163.
- 30. A. Kitada, S. Takeoka, K. Kintsu, K. Fukami, M. Saimura, T. Nagata, M. Katahira and K. Murase, *Journal of The Electrochemical Society*, 2018, **165**, H121-H127.
- 31. P. Batamack and J. Fraissard, *Catalysis letters*, 1995, **35**, 135-142.
- 32. B. Antalek, *Concepts in Magnetic Resonance*, 2002, **14**, 225-258.
- 33. H. Nakamoto, A. Noda, K. Hayamizu, S. Hayashi, H.-o. Hamaguchi and M. Watanabe, *The Journal of Physical Chemistry C*, 2007, **111**, 1541-1548.
- 34. J. Hou, Z. Zhang and L. A. Madsen, *J Phys Chem B*, 2011, **115**, 4576-4582.
- 35. N. Yaghini, M. N. Garaga and A. Martinelli, Fuel Cells, 2016, 16, 46-54.
- 36. N. Yaghini, L. Nordstierna and A. Martinelli, Phys Chem Chem Phys, 2014, 16, 9266-9275.